



POLİTEKNİK DERGİSİ

JOURNAL of POLYTECHNIC

ISSN: 1302-0900 (PRINT), ISSN: 2147-9429 (ONLINE)

URL: <http://dergipark.org.tr/politeknik>



Design of a GaN-Based high-frequency inverter for electrosurgery.

Elektrocerrahi için GaN tabanlı yüksek frekanslı bir inverter tasarımı

Yazar(lar) (Author(s)): Hale TARINC¹, Sevilay CETIN²

ORCID¹: 0000-0001-6217-2041

ORCID²: 0000-0002-9747-4821

To cite to this article: Abuşka M., Akgül M. B. ve Altıntaş V., “Yutucu plaka üzerine konik yayların yerleştirildiği güneş enerjili hava kollektörünün bulanık mantık ile modellenmesi”, *Journal of Polytechnic*, *(*) : *, (*).

Bu makaleye şu şekilde atıfta bulunabilirsiniz: Abuşka M., Akgül M. B. ve Altıntaş V., “Yutucu plaka üzerine konik yayların yerleştirildiği güneş enerjili hava kollektörünün bulanık mantık ile modellenmesi”, *Politeknik Dergisi*, *(*) : *, (*).

Erişim linki (To link to this article): <http://dergipark.org.tr/politeknik/archive>

DOI: 10.2339/politeknik.1424645

Design of A GaN-Based High-Frequency Inverter for Electrosurgery

Highlights

- ❖ Electrosurgery
- ❖ High Frequency
- ❖ Resonant Inverter

Graphical Abstract

In this work presents the design of a class dual-ended (DE) resonant inverter with gallium nitride (GaN) based high-frequency and full-bridge topology for electrosurgery.

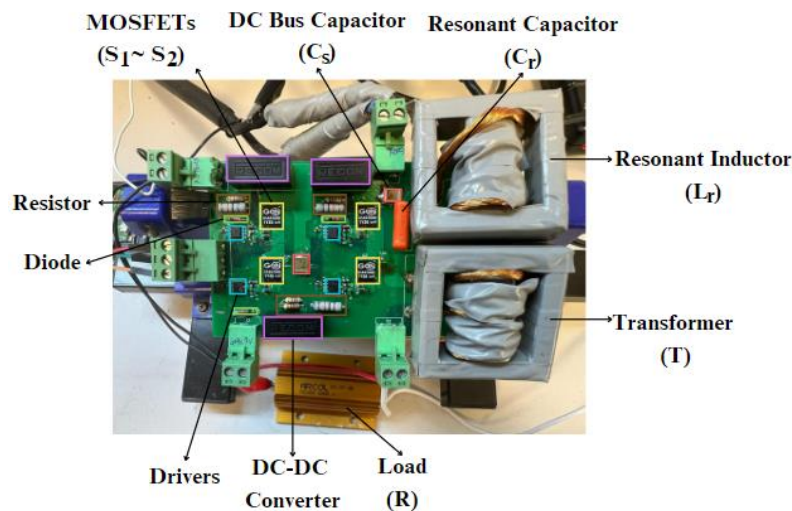


Figure. Prototype design built in the laboratory

Aim

The aim of this work is to design a GaN-based high-frequency full-bridge class DE resonant inverter topology for electrosurgery.

Design & Methodology

High-frequency and wide load range are taken into consideration in the design procedure. The selected switching frequency is 500 kHz. Variable loads are applied to the designed inverter and measurements are taken.

Originality

In this study, a high-frequency full-bridge class DE resonant inverter operating in a wide load range for three modes of electrosurgery applications is designed.

Findings

The presented design is verified on a prototype and results are obtained for all three modes, pure cutting, blend, and coagulation, at variable loads. In addition, studies have been carried out on a different load simulating real tissue for all three modes.

Conclusion

A high-frequency inverter design operating at wide load range has been obtained for electrosurgery. On the potato load for pure cutting mode, an output voltage of 39.9 V and an output current of 0.7 A while the efficiency is around 35%.

Declaration of Ethical Standards

The author(s) of this article declare that the materials and methods used in this study do not require ethical committee permission and/or legal-special permission.

Design of A GaN-Based High-Frequency Inverter for Electrosurgery

Araştırma Makalesi / Research Article

Hale TARINC^{1*}, Sevilay CETİN²

¹Department of Biomedical Engineering Technology Faculty, Pamukkale University, Turkey

(Geliş/Received : 23.01.2024 ; Kabul/Accepted : 15.04.2024 ; Erken Görünüm/Early View : 20.05.2024)

ABSTRACT

Electrosurgery performs cutting and coagulation procedures using high-energy and high-frequency electric current. It reduces bleeding during surgical interventions, shortens the operation time, and accelerates the healing process. In this study, a GaN-based high-frequency full-bridge class DE resonant inverter design is proposed for use in electrosurgery. The proposed inverter provides AC voltage at high frequencies and the switches operate with zero voltage switching (ZVS) at low voltage stress. In addition, the use of GaN elements provides operation in wide bandwidth, high frequency, and low switching losses. The switching frequency is selected as 500 kHz for three different cutting modes of electrosurgery. After the theoretical analysis and simulation studies of the proposed inverter, an experimental setup was designed and implemented in a laboratory environment. The efficiency performance over a variable load range is analysed. Finally, three modes of electrosurgery (pure cutting, blend, coagulation) are tested on the different loads, potato - chicken breast - liver, simulating real tissue. On the potato load for pure cutting mode, an output voltage of 39.9 V and an output current of 0.7 A while an efficiency of 35%.

Keywords: electrosurgery, high frequency, GaN, resonant inverter.

Elektrocerrahi için GaN Tabanlı Yüksek Frekanslı Bir Inverter Tasarımı

ÖZ

Elektrocerrahi, yüksek enerji ve yüksek frekanslı elektrik akımı kullanarak kesme ve pıhtılaşma işlemlerini gerçekleştirir. Cerrahi müdahalelerde kanamayı azaltır, operasyon süresini kısaltır ve iyileşme sürecini hızlandırır. Bu çalışmada elektrocerrahide kullanılmak üzere GaN tabanlı yüksek frekanslı tam köprü DE sınıfı rezonans inverter tasarımı önerilmektedir. Önerilen dönüştürücü yüksek frekanslarda AC gerilim sağlamakta ve anahtarlar düşük gerilim stresinde sıfır gerilim anahtarlama (ZVS) ile çalışmaktadır. Ayrıca GaN elemanların kullanımı geniş bant aralığında, yüksek frekansta ve düşük anahtarlama kayıplarında çalışmasını sağlar. Elektrocerrahinin üç farklı kesme modu için anahtarlama frekansı 500 kHz olarak seçilmiştir. Önerilen inverterin teorik analiz ve simülasyon çalışmalarının ardından bir deney düzeneği tasarlanmış ve laboratuvar ortamında uygulanmıştır. Değişken bir yük aralığında verimlilik performansını analiz edilmiştir. Son olarak, elektrocerrahinin üç modu (saf kesme, karışık kesme, koagülasyon) gerçek dokuyu simüle eden patates - tavuk göğsü - karaciğer gibi farklı yükler üzerinde test edilmiştir. Saf kesme modu için patates yükünde, çıkış gerilimi 39,9 V ve çıkış akımı 0,7 A iken verimlilik %35'tir.

Anahtar Kelimeler: elektrocerrahi, yüksek frekans, GaN, rezonans inverter.

1. INTRODUCTION

William T. Bovie popularized Electrosurgery. Between 1914 and 1927, he developed the first electrosurgical device in the frequency range of 250 kHz-2 MHz. It was later accepted by surgeons [1].

Electrosurgery, which is important in the field of surgery, enables the energy to be transmitted from the device to the tissue by manual adjustment by the doctor. The transmitted energy is adjusted according to the clinical impact and actual human tissue type [2].

Electrosurgery is divided into monopolar electrosurgery and bipolar electrosurgery. The main difference between the two modes is the method of the tissue. Two electrodes

are used in monopolar electrosurgery, an active and a neutral electrode, while bipolar electrosurgery uses the forceps electrode [3,4]. The monopolar electrosurgery structure can be shown in Figure 1. The active electrode has a small surface area and the current density around it is high. On the other hand, the neutral electrode with a large surface area minimizes heating in the area and is placed away from the active electrode to safely distribute the current [5].

Electrosurgery has pure cutting, blend, and coagulation modes. For pure cutting mode, current and voltage are a continuous sine. Blend performs both pure cutting and coagulation, so it needs to give a modulated waveform. For coagulation, it gives a sudden sine output [2], [6], [7]. The modes of electrosurgery provide the desired clinical effect for the surgical operation. To achieve this, it generates signals with a lower limit frequency of 200 kHz and an upper limit frequency of 5 MHz [8]. An alternating current above 200 kHz is applied to avoid

*Sorumlu Yazar (Corresponding Author)
e-posta : tarinchale@gmail.com

muscle stimulation [9]. This is why electrosurgical devices are designed in this way.

Human has different tissue impedances such as skin, muscle, and fat [2], [10]. During surgery operation, the tissue load changes across a broad spectrum, and the output power must be maintained [11]. Therefore, high-frequency AC output voltage with a wide range variable load is required for electrosurgery [2], [11].

Switching losses can be minimized in high-frequency resonant converter topologies [12]. High-frequency resonant inverters are usually used in electrosurgery applications [13]. Among the resonant inverters, class D, class E, and class DE are commonly used resonant inverters [11]. Class D resonant inverters are preferred for high-voltage applications [14], [15] and their switching current voltage stress is low [11], [16]. When inductive only, turn-on switching losses are zero while turn-off transition is hard. Therefore, switching losses are high, meaning efficiency is low [17]. Class E resonant inverters work with ZVS, so efficiency is high and they are low cost because there is a single switch in the circuit. However, it has high current and voltage stress [11], [17]-[19]. Class DE resonant inverters include the advantages of both class D and class E resonant inverters. Therefore, it has no switching power losses and provided ZVS, that is, it operates at high efficiency and the switch current voltage stresses are low [11], [17], [20]-[22].

Looking at recent studies for electrosurgery, a 2018 study proposed the design of a high-frequency pulse width modulation (PWM) half-bridge inverter for electrosurgery cutting applications and tested it on chicken tissue [23]. In the 2021 study, only the pure cutting mode of electrosurgery was examined and two-stage power conversion was proposed to provide output voltage regulation over a wide range. These stages are resonant single-ended primary inductor converter (SEPIC) and class DE resonant inverter, respectively [11]. In a similar study conducted in 2022, a high-frequency voltage inverter combining half-bridge and full-bridge operations is recommended so the proposed inverter provides wide-range voltage regulation for electrosurgery [24]. The half-bridge inverter operating mode is activated for minor surgical applications for example coagulation. For large surgical applications for example pure cutting, the full-bridge inverter operating mode is turn-on. In another study, a phase-shifted gallium nitride high electron mobility transistor (GaN HEMT) based full-bridge very high-frequency AC inverter (VHFI) providing three operation modes of electrosurgery was proposed to power electrosurgery [2].

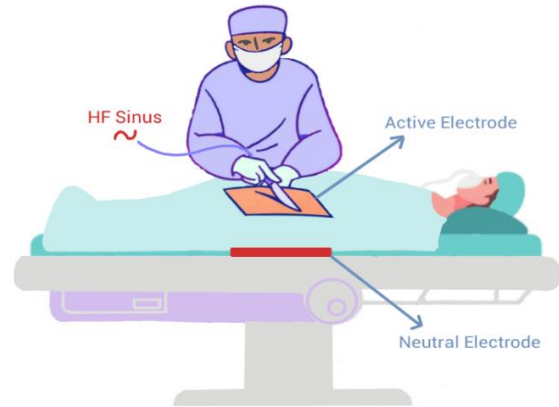


Figure 1. The monopolar electrosurgery structure

In this study, GaN-based high-frequency class DE resonant inverter topology was chosen, considering the advantages mentioned earlier. According to current knowledge of authors, class DE resonant inverter is usually used for pure cutting mode of electrosurgery in literature. Therefore, in this work, three modes of electrosurgery (pure cutting, blend, coagulation) were examined and efficiency results were evaluated. In addition, the cutting results of the three modes were also observed on the different loads, which are potato, chicken breast, and liver, to simulate real tissue. As a result, in this work, a high-frequency full-bridge class DE resonant inverter operating in a wide load range for three modes of electrosurgery applications is designed.

2. OPERATING STATES OF THE PROPOSED INVERTER

The schematic diagram of the proposed inverter is given in Figure 2. It includes a voltage source (V_{in}), MOSFETs ($S_1 \sim S_4$), capacitors ($C_1 \sim C_4$) connected in parallel with the MOSFETs, a series resonant (C_r, L_r), a transformer (T) with a 1:1 turns ratio (n) to isolation the circuit, and a load (R).

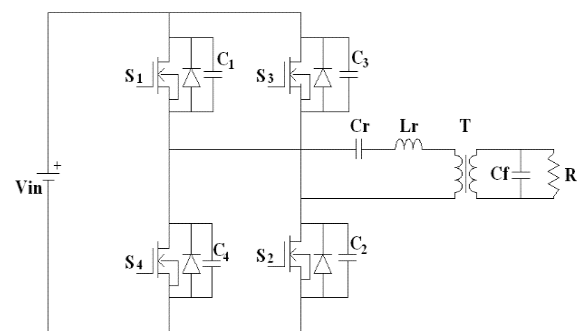


Figure 2. The full-bridge class DE resonant inverter.

In order to reduce the switch current voltage stress, the class DE resonant inverter is a full-bridge structure. There is a certain period of dead time between the switches to ensure ZVS. The operating conditions of the proposed inverter at the time intervals are given in Figure

3 and the waveforms of the time intervals are given in Figure 4.

$[t_0, t_1]$: Switches $S_1 - S_2$ are turn-on. The resonant current flows through these two switches and the resonant begins between the resonant elements ($C_r - L_r$). It is shown in Figure 3 (a).

$[t_1, t_2]$: During the time interval given in Figure 3 (b), switches $S_1 - S_2$ are turn off and capacitors $C_1 - C_2$ connected in parallel to these switches begin to charge. At the same time, capacitors $C_3 - C_4$ are completely discharged, and switches $S_3 - S_4$ turn ZVS on.

$[t_2, t_3]$: Switches $S_3 - S_4$ are in turn on. This time the resonant current flows through these two switches. The resonant begins between the resonant elements ($C_r - L_r$). It is given in Figure 3 (c).

$[t_3, t_4]$: During the time interval given in Figure 3 (d), switches $S_3 - S_4$ turn off and capacitors $C_3 - C_4$ connected in parallel to these switches begin to charge. At the same time, capacitors $C_1 - C_2$ are completely discharged, and switches $S_1 - S_2$ turn on with ZVS again.

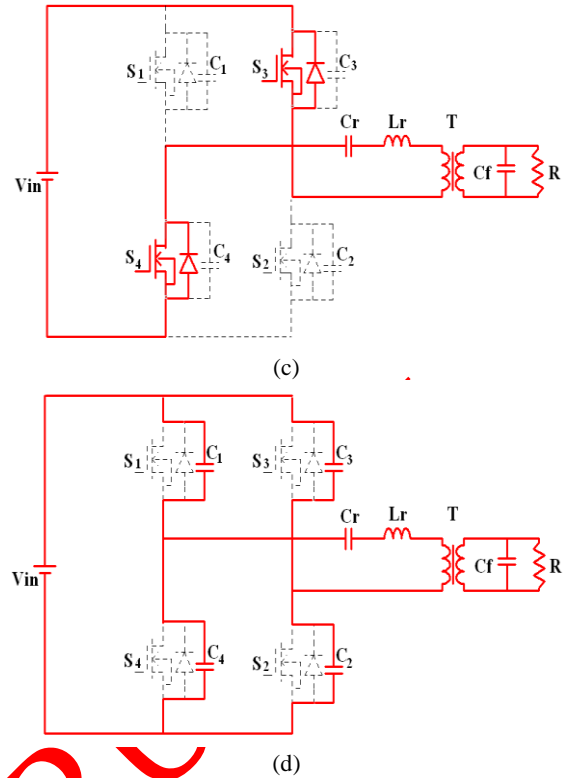
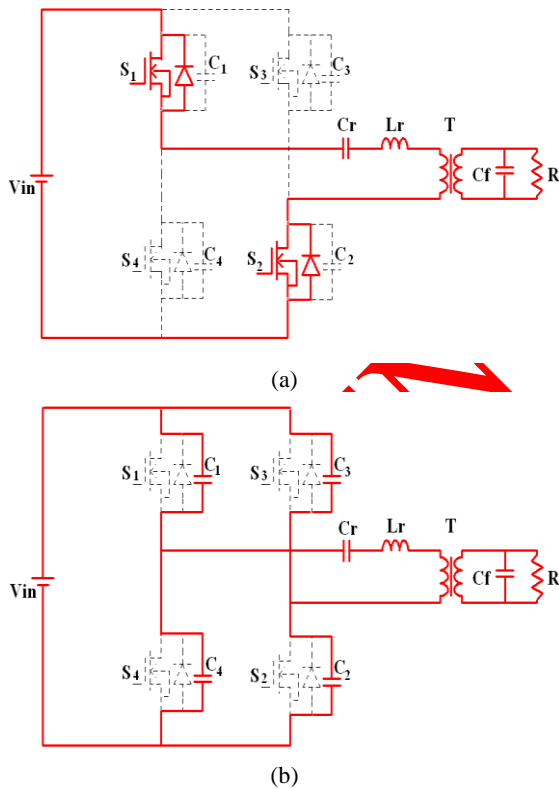


Figure 3. Operating states of full-bridge class DE resonant inverter. (a) $[t_0, t_1]$, (b) $[t_1, t_2]$, (c) $[t_2, t_3]$, (d) $[t_3, t_4]$

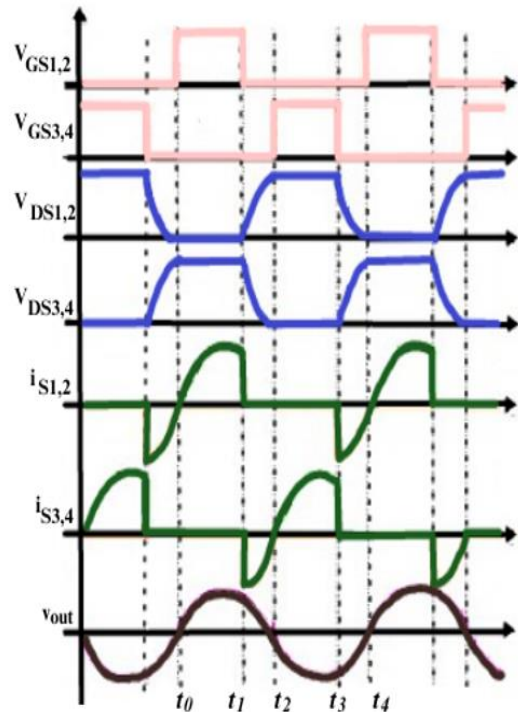


Figure 4. Waveforms of the operation of the proposed inverter

The resonant frequency of the inverter circuit can be extracted as:

$$f_r = \frac{1}{2\pi\sqrt{L_r C_r}} \quad (1)$$

The expressions for the capacitance and inductance of the capacitor and inductor that provide series resonant are C_r and L_r respectively. It is calculated by the equation below.

$$C_r = \frac{1}{\omega R(Q - \frac{\pi}{2})} \quad (2)$$

$$L_r = \frac{QR}{\omega} \quad (3)$$

The high preferred quality factor for a good total harmonic distortion (THD) can be found in the equation below.

$$Q = \frac{\omega L_r}{R} = \frac{1}{\omega C_r R} = \frac{Z_o}{R} = \sqrt{\frac{L_r}{C_r}} \quad (4)$$

In this equation, ω represents the angular frequency and the resonance impedance value is Z_o .

In a full-bridge class DE resonant inverter, there are four parasitic capacitors of MOSFETs in the form $C=C_1=C_2=C_3=C_4$. These capacitors are located between the drain-source terminals of the MOSFETs and affect the operation of the MOSFET. It can be calculated by the following equation:

$$C = C_1 = C_2 = C_3 = C_4 = \frac{1}{4\pi^2 R_{\max} f_{\max}} \quad (5)$$

Output power and efficiency can be found by the following equations:

$$P_o = \frac{V_o^2}{R} \quad (6)$$

$$\eta = \frac{P_o}{P_i} \quad (7)$$

3. SIMULATION AND EXPERIMENTAL RESULTS

3.1. Simulation Results

In this study, a simulation study was performed first. The full-bridge class DE resonant inverter design, which realizes three modes for electrosurgery has been simulated and shown in Figure 5. The switching frequency of the circuit is selected as 500 kHz. A variable load range is used in the study as in the same tissue and the input voltage is 200 V. The three modes of electrosurgery are considered separately.

The values of the components used in the simulated circuit diagram (Figure 5) are shown in Table 1. GaN

MOSFET is used because GaN devices operate in wide bandwidth, high frequency, high power, low switching losses, and high performance [25]-[30].

Table 1. Parameters and specification

Circuit Parameters	Symbol	Value
Switch	$S_1 \sim S_4$	GS66508B
Input Voltage	V_{in}	200 V
Switching frequency	f_{sw}	500 kHz
Resonant capacitor	C_r	4 nF
Resonant inductor	L_r	72 μ H
Load resistor	R	50 $\Omega \sim$ 300 Ω
Transformer turns ratio	n	1:1

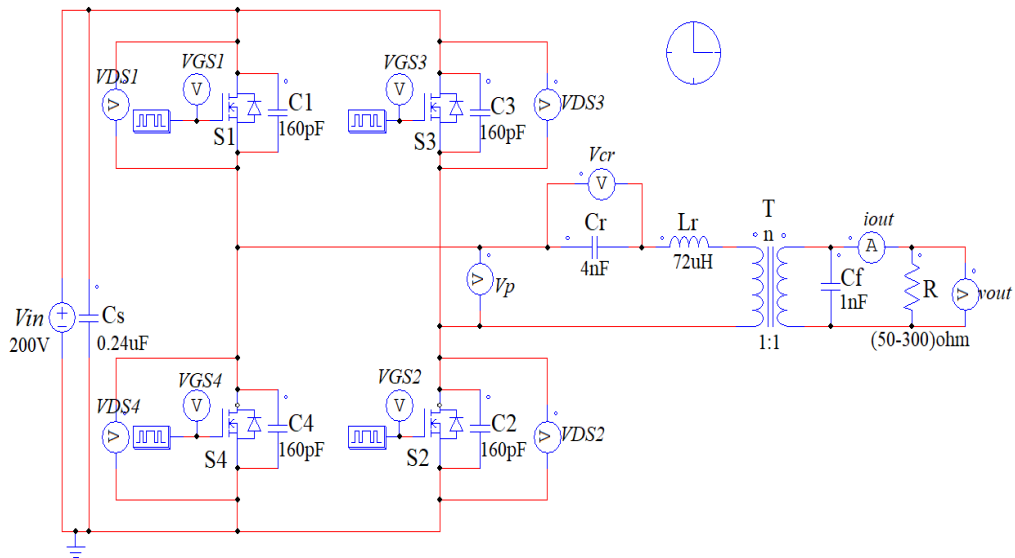


Figure 5. The simulated circuit of the proposed inverter

At a switching frequency of 500kHz, the switches in the cross arm ($S_1 - S_2$, $S_3 - S_4$) are being transmitted simultaneously, and the results of the waveforms providing ZVS for switches $S_2 - S_3$ are shown in Figure 6.

The simulation waveforms of the pure cutting mode are given in Figure 7. At 500 kHz switching frequency, at 100 Ω load, are obtained. In addition, the primary voltage (V_p), the resonant capacitor voltage (V_{cr}), continuous sine output voltage (V_{out}) and output current (i_{out}) are obtained respectively.

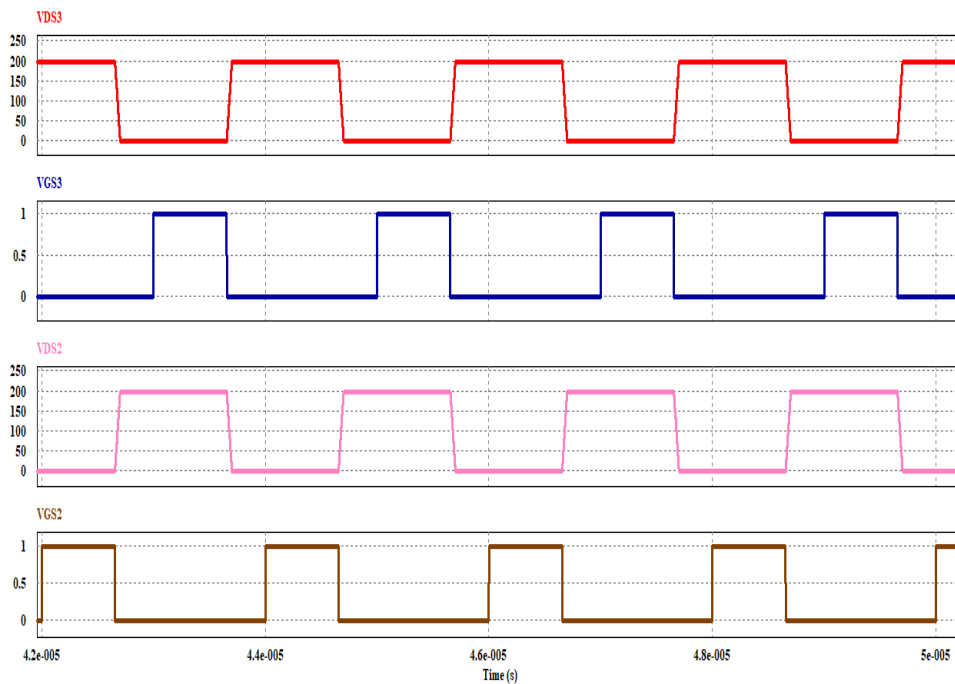


Figure 6. The ZVS waveform of the S_2 and S_3 switches

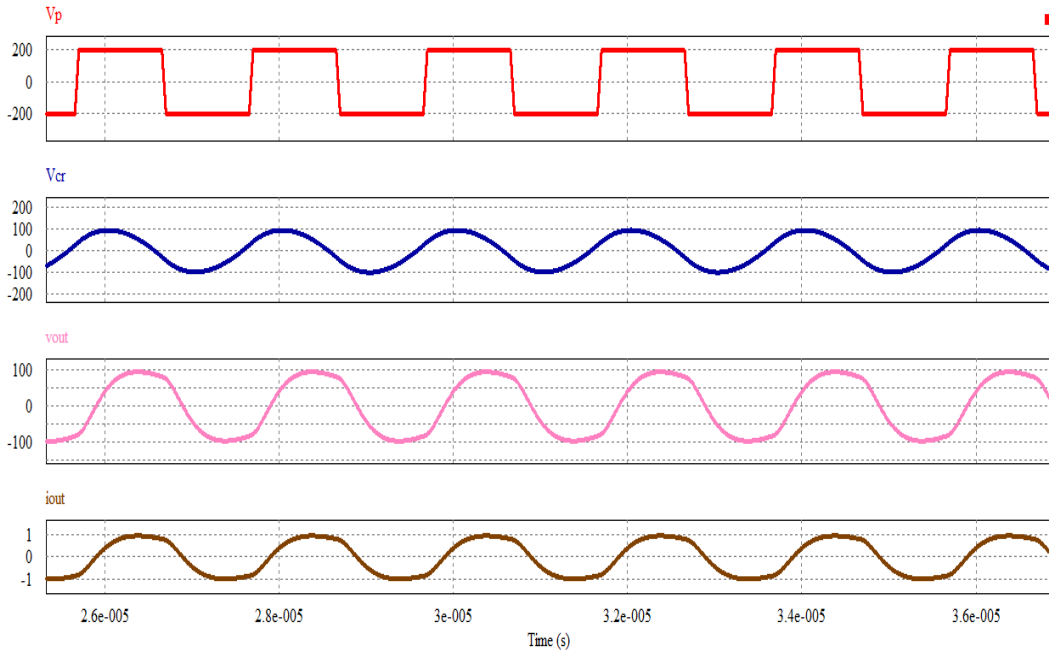


Figure 7. Waveforms for pure cutting mode. Primary voltage V_p , resonant capacitor voltage V_{cr} , output voltage v_{out} , and output current i_{out}

Blend, unlike pure cutting mode, involves a modulated waveform. Using the catalog of Force FXTM-C [7] electro-surgical device, the repeated frequency is set to 27 kHz. The output voltage and output current at 100 Ω are given in Figure 8.

Coagulation provides a sudden sine output voltage. Using the catalog of Force FXTM-C [7] electro-surgical device, the repeated frequency is set to 39 kHz, and the output voltage and output current at 100 Ω are given in Figure 9.

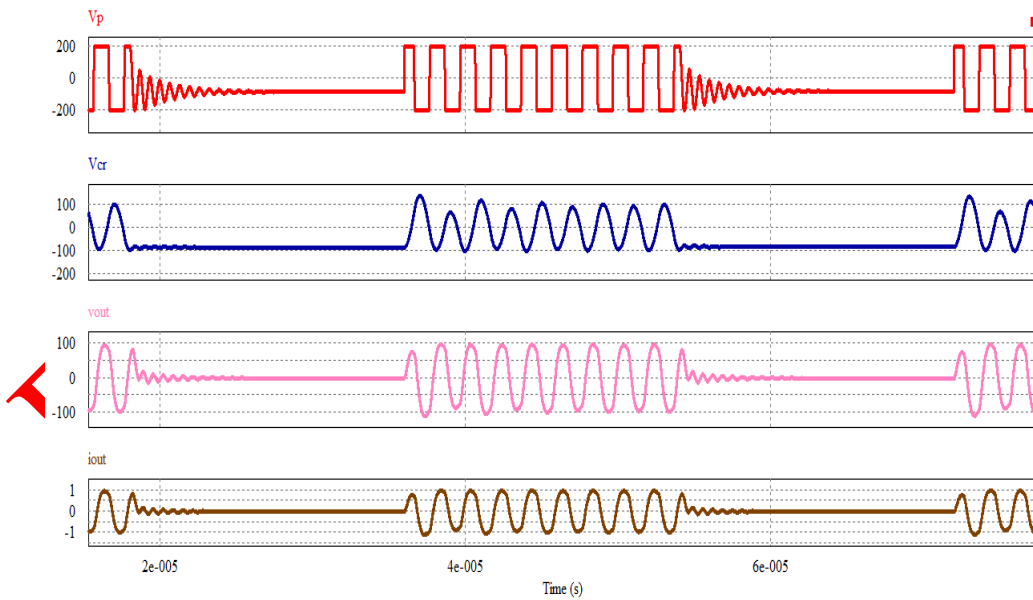


Figure 8. Waveforms for blend mode. Primary voltage V_p , resonant capacitor voltage V_{cr} , output voltage v_{out} , and output current i_{out}

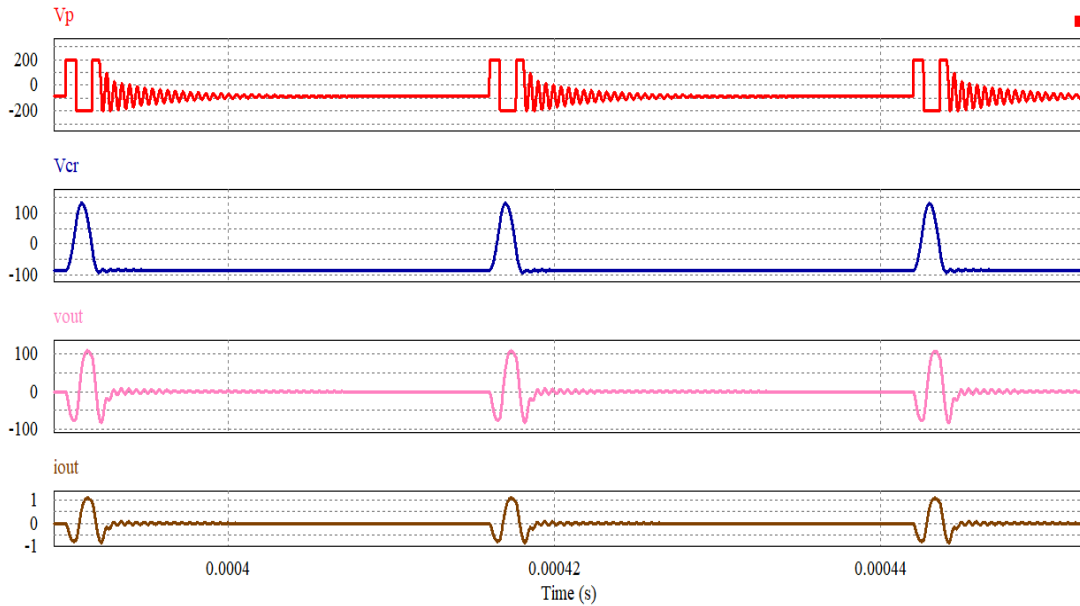


Figure 9. Waveforms for coagulation mode. Primary voltage V_p , resonant capacitor voltage V_{cr} , output voltage v_{out} , and output current i_{out}

3.2. Experimental Results

The simulation results are evaluated and based on these results a prototype is built in the laboratory. The prototype is built considering the design parameters shown in Table 1 and the picture of the built prototype is given in Figure 10.

The control circuit is designed as open loop and the control signals are produced with STM32 microcontroller. In order to guarantee ZVS operation, class DE resonant inverter is designed to operate inductive region which is possible switching frequency is higher than resonant frequency.

The experimental results of the ZVS waveforms of S_2 and S_3 GaN MOSFETs at $100\ \Omega$ load are given in Figure 11.

Figure 12 gives the experimental results for electrosurgery at $100\ \Omega$ load for three modes.

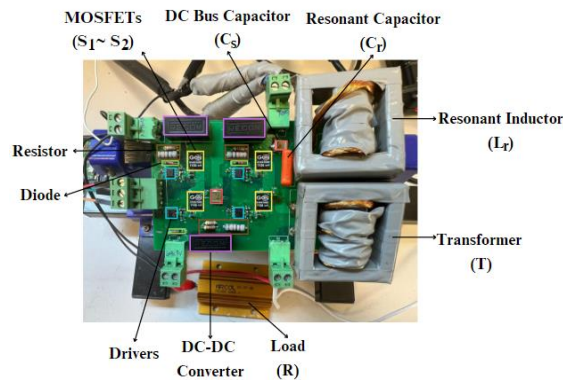


Figure 10. Prototype design built in the laboratory

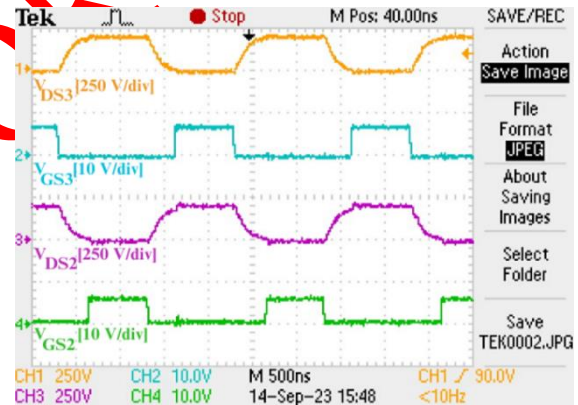
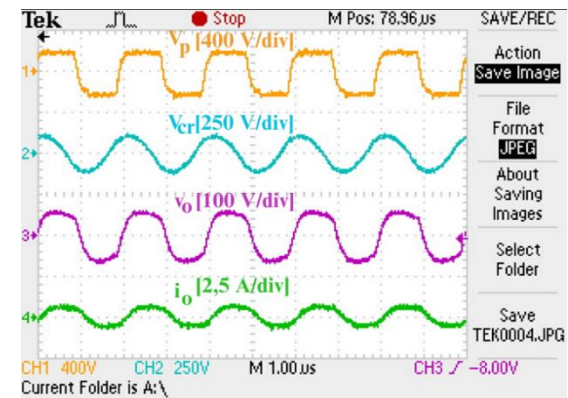
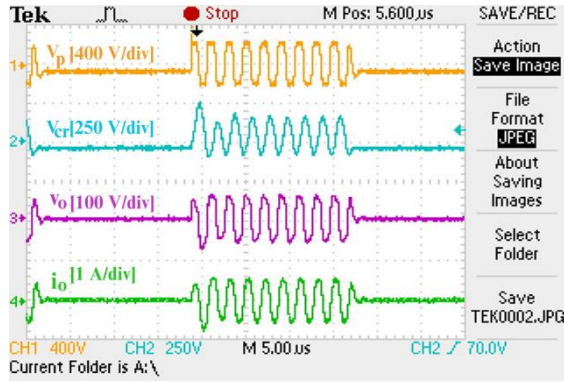


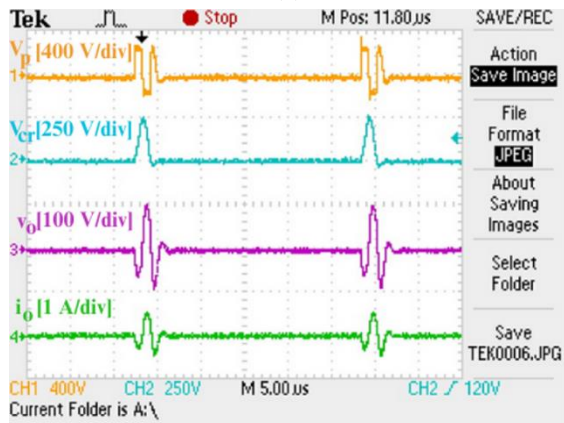
Figure 11. ZVS waveform of S_2 and S_3 GaN MOSFETs in the experimental environment



(a)



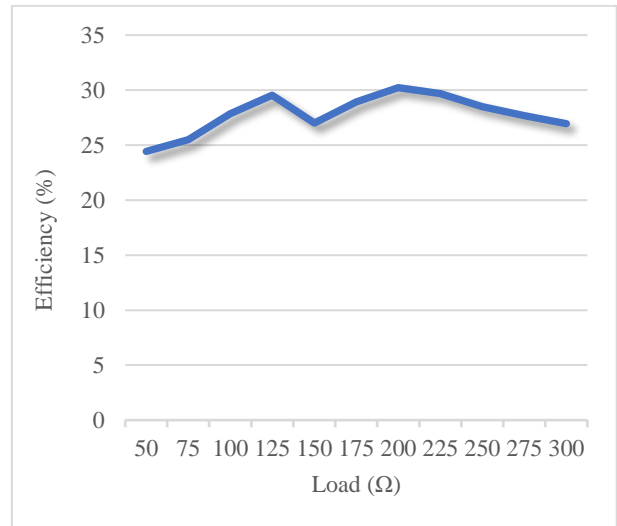
(b)



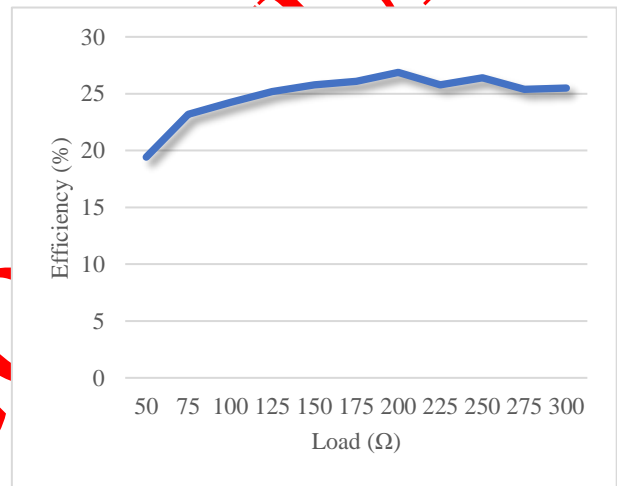
(c)

Figure 12. The experimental results of inverter for electrosurgery at 100 Ω load. (a) pure cutting, (b) blend, (c) coagulation

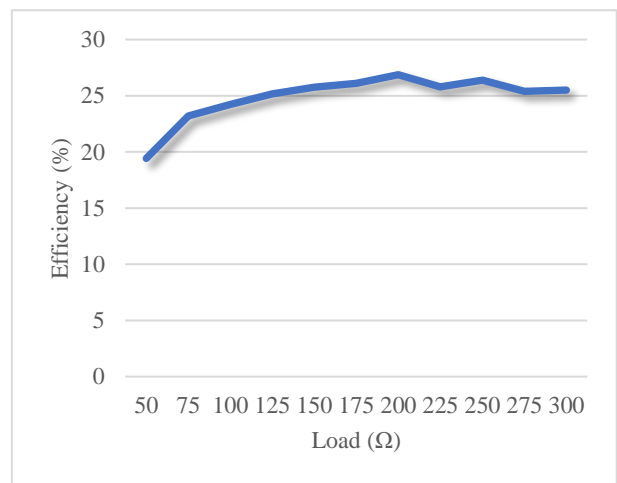
The efficiency graphs were extracted for all three modes with equations (6) and (7) using measured current and voltage values in the variable load range of 50 Ω ~ 300 Ω . At 200 V input voltage, the efficiency values obtained at different load values are shown in Figure 13. An output power of about 22 W has been achieved at 200 Ω load for pure cutting mode and the maximum efficiency is measured around 30%. For pure cutting mode, the maximum efficiency is obtained as 35% on the potato load while an output voltage of 39.9 V and an output current of 0.7 A. The cutting modes on the potato is shown in Figure 14. The output power of the built prototype is around 22 W and the losses independent of the load such as core losses dominated in the total power losses. Thus, the efficiency is low due to low power rate.



(a)



(b)



(c)

Figure 13. Efficiency graph over a variable load range. (a) pure cutting, (b) blend, (c) coagulation

In addition, the built prototype is also tested on the chicken breast, and the liver loads to validate its performance. The cutting modes on the chicken breast

and liver are given in Figure 15 and Figure 16, respectively.



Figure 14. Cutting results on the potato



Figure 15. Cutting results on the chicken breast



Figure 16. Cutting results on the liver

4. CONCLUSION

In this paper, a GaN-based high-frequency full-bridge class DE resonant inverter is designed for electrosurgery. The selected switching frequency is 500 kHz, considering the switching frequency of the electrosurgical devices used. The design procedure of the proposed inverter is based on the methods in the literatures. The circuit design is simulated and a prototype is built in the laboratory. It is tested for pure cutting, blend, and coagulation modes. Each operating

state's performance was evaluated by measuring the efficiency over a specified load range ($50 \Omega \sim 300 \Omega$). Finally, cutting operations were performed on potato, chicken breast, and liver for all three operating modes.

ACKNOWLEDGEMENT

This work is supported by Pamukkale University under grant number 2022FEBE042.

DECLARATION OF ETHICAL STANDARDS

The author(s) of this article declare that the materials and methods used in this study do not require ethical committee permission and/or legal-special permission.

AUTHORS' CONTRIBUTIONS

Hale TARINÇ: She contributed to the literature research, analysis and built the prototype of a high-frequency full-bridge class DE resonant inverter.

Sevilay ÇETİN: She contributed to the management of all stages.

CONFLICT OF INTEREST

There is no conflict of interest in this study.

REFERENCES

- [1] Ramachandran M., & Aronson J. K., "John Marshall's first description of surgical electrocautery," *Journal of the Royal Society of Medicine*, 104(9): 355-360 (2011). doi:10.1258/jrsm.2011.11k028.
- [2] Bao C. and Mazumder S. K., "GaN-HEMT Based Very-High-Frequency AC Power Supply for Electrosurgery", *2021 IEEE Applied Power Electronics Conference and Exposition (APEC)*, 220-225, (2021). doi:10.1109/APEC42165.2021.9487352.
- [3] Eggleston J. L., & Maltzahn W. W., "Electrosurgical Devices", (ed: Bronzino J. D.), *Medical Devices and Systems*, Taylor & Francis Group, 63: 2-9, Boca Raton (2006).
- [4] Ozdemir U., "Is electrosurgery a revolution? Mechanism, benefits, complications and precautions", *J Pharm Technol*, 1(3): 60-64, (2020). doi: 10.37662/jpt.2021.8.
- [5] Petrova G., Yanev G., and Spasov G., "Arduino-based module for return electrode contact quality monitoring in the electrosurgical instruments," *2017 XXVI International Scientific Conference Electronics (ET)*, Sozopol, Bulgaria, 1-4, (2017). doi: 10.1109/ET.2017.8124379.
- [6] Tarinc H. and Cetin S., "Efficiency Performance Evaluation of A Second Stage GaN Based High Frequency Inverter for Electrosurgery," *2023 14th International Conference on Electrical and Electronics Engineering (ELECO)*, Bursa, Turkey, 1-5, (2023). doi: 10.1109/ELECO60389.2023.10416039.
- [7] "User's Guide Force FXTM-C Electrosurgical Generator with Instant ResponseTM Technology." 2000. Accessed: Aug, 23, 2023. [Online]. Available: <http://www.frankshospitalworkshop.com>.
- [8] Bao C. and Mazumder S. K., "Multiresonant-Frequency Filter for an Electrosurgery Inverter," *IEEE Transactions on Power Electronics*, 37(6): 6242-6246, (2022). doi: 10.1109/TPEL.2021.3137525.
- [9] Advincula A. P., Wang K. "The evolutionary state of electrosurgery: where are we now?" *Current Opinion Obstetrics and Gynecology*. 20(4): 353-8 (2008). doi: 10.1097/GCO.0b013e3283073ab7.
- [10] Schneider B. and Abatti P. J., "Electrical Characteristics of the Sparks Produced by Electrosurgical Devices," *IEEE Transactions on Biomedical Engineering*, 55(2): 589-593, (2008). doi: 10.1109/TBME.2007.903525.
- [11] Gu L., & Wang L., "Two-stage wide-output high-frequency-voltage inverter for electrosurgical generator," *IECON 2021 – 47th Annual Conference of the IEEE Industrial Electronics Society*, Toronto, ON, Canada, 1-6, (2021). doi: 10.1109/IECON48115.2021.9589891.
- [12] Corak İ. & Cetin S., "8 MHz High Efficient Resonant SEPIC Converter Design for LED Driver of Endoscopy Systems", *Journal of Polytechnic*, 27(2): 461-468, (2024). doi: 10.2339/politeknik.1118158.
- [13] Jensen S., Corradini L., Rodríguez M., & Maksimovic D., "Modeling and digital control of LCLC resonant inverter with varying load", *2011 IEEE Energy Conversion Congress and Exposition*, (2011). doi: 10.1109/ECCE.2011.6064288.
- [14] Park N. -J., Lee D. -Y. and Hyun D. -S., "A Power-Control Scheme With Constant Switching Frequency in Class-D Inverter for Induction-Heating Jar Application," *IEEE Transactions on Industrial Electronics*, 54 (3): 1252-1260 (2007). doi: 10.1109/TIE.2007.892741.
- [15] Jittakort J., Nimsontorn J., Sirboonrueng B., Chua-on S., Pinpathomrat P. and Chudjarjeen S., "A Class D Voltage Source Resonant Inverter for Ultrasonic Cleaning Application," *2018 International Conference on Engineering, Applied Sciences, and Technology (ICEAST)*, Phuket, Thailand, 1-4, (2018). doi: 10.1109/ICEAST.2018.8434484.
- [16] Tebianian H., Salami Y., Jeyasurya B. and Quaicoe J. E., "A 13.56-MHz Full-Bridge Class-D ZVS Inverter With Dynamic Dead-Time Control for Wireless Power Transfer Systems," in *IEEE Transactions on Industrial Electronics*, 67(2): 1487-1497, (2020). doi: 10.1109/TIE.2018.2890505.
- [17] Kazimierczuk M. K., and Czarkowski D., "Resonant Power Converters", *John Wiley & Sons*, 141-404, Canada, (2011).
- [18] Mazumder S. K., Bao C., El-Kebir H., Lee Y., Bentsman J., and Berlin R., "Electrosurgery Power Electronics: A Revolution in the Making," *2023 IEEE Applied Power Electronics Conference and Exposition (APEC)*, Orlando, FL, USA, 692-698, (2023). doi: 10.1109/APEC43580.2023.10131328.
- [19] Ashique RH, Shihavuddin ASM, Khan MM, Islam A, Ahmed J, Arif MSB, Maruf MH, Al Mansur A, Haq MAu, and Siddiquee A, "An Analysis and Modeling of the Class-E Inverter for ZVS/ZVDS at Any Duty Ratio with High Input Ripple Current," *Electronics*, 10(11): 1312, (2021). <https://doi.org/10.3390/electronics10111312>.
- [20] Sekiya H., Miyahara R., and Kazimierczuk M. K., "Design of class-DE amplifier with linear and nonlinear shunt capacitances for 25 % duty ratio," *2009 IEEE International Symposium on Circuits and Systems (ISCAS)*, Taipei, Taiwan, 2870-2873, (2009). doi: 10.1109/ISCAS.2009.5118401.
- [21] Kondo T., Inaba T., Sakai Y., and Koizumi H., "An Analysis of Class DE Voltage-Source Parallel Resonant Inverter," *2018 International Power Electronics Conference (IPEC-Niigata 2018 -ECCE Asia)*, Niigata, Japan, 4114-4121, (2018). doi: 10.23919/IPEC.2018.8507504.

- [22] Wang P, Li Q, Liu Y, Yuan W, Yan K, Pang Z. "A Novel Impedance Matching of Class DE Inverter for High Efficiency, Wide Impedance WPT System", *Electronics*, 13(5): 959, (2024). <https://doi.org/10.3390/electronics13050959>.
- [23] Sanajit N. & Meesrisuk W., "A High-Frequency PWM Half-Bridge Inverter for Electrosurgical Cutting Applications," *2018 21st International Conference on Electrical Machines and Systems (ICEMS)*, Jeju, Korea (South), 827-830, (2018). doi: 10.23919/ICEMS.2018.8549089.
- [24] Liu L., Li Y. & Gu L., "Multiphase Interleaved Reconfigurable High-Frequency-Voltage Inverter for Electrosurgical Generator," *2022 IEEE Energy Conversion Congress and Exposition (ECCE)*, Detroit, MI, USA, 1-5, (2022). doi: 10.1109/ECCE50734.2022.9947632.
- [25] Husna H, K., & Nirmal, D. "A Review of GaN HEMT BroadBand Power Amplifiers," *AEU - International Journal of Electronics and Communications*, 153040, (2020). doi:10.1016/j.aeue.2019.153040.
- [26] Hu J., Zhang Y., Sun M., and Piedra D., Chowdhury, N., & Palacios, T. "Materials and processing issues in vertical GaN power electronics" *Materials Science in Semiconductor Processing*, 78: 75–84, (2018). doi:10.1016/j.mssp.2017.09.033.
- [27] Khan S. A., Wang M., and Chaturvedi S., "Analog Resistive Sensing Control for GaN FET's based Totem Pole PFC," *2023 IEEE Design Methodologies Conference (DMC)*, Miami, FL, USA, 1-5, (2023). doi: 10.1109/DMC58182.2023.10412551.
- [28] Yang S., Han S., Sheng K. & Chen K. J., "Dynamic On-Resistance in GaN Power Devices: Mechanisms, Characterizations, and Modeling," in *IEEE Journal of Emerging and Selected Topics in Power Electronics*, 7 (3): 1425-1439, (2019). doi: 10.1109/JESTPE.2019.2925117.
- [29] Bilgili A. K., Hekin E., Ozturk M., Ozcelik S., & Ozbay E., "Mosaic Defect and AFM Study on GaN/AlInN/AlN/Sapphire HEMT Structures", *Journal of Polytechnic*, 25(4): 1613–1619, (2022). doi: 10.2339/politeknik.787700.
- [30] Tugrul D., Cakmak H., Ozbay E., & Imer B., "Development of AZO TCOs with ALD for HEMT and HJSC Solar Cell Applications", *Journal of Polytechnic*, 26,(1): 209–214, (2023). doi: 10.2339/politeknik.873160.